Available online at www.sciencedirect.com
SCIENCE DIRECT
Tetrahedron
Tetrahedron 62 (2006) 6574–6580

Externally sensitized mesolytic fragmentations in dithiane–ketone adducts

Tiffany P. Gustafson, Alexei N. Kurchan and Andrei G. Kutateladze*

Department of Chemistry and Biochemistry, University of Denver, Denver, CO 80208-2436, USA

Received 11 September 2005; accepted 12 November 2005
Available online 17 April 2006

Abstract—The apparent activation enthalpies, $\Delta H^{\neq}$, for externally sensitized mesolytic fragmentations in benzophenone–dithiane adducts were obtained in variable temperature photolyses and compared with DFT activation barriers calculated for β-scission in the corresponding oxygen-centered radicals. The results of these experimental and theoretical studies further support the mechanism in which deprotonation of the hydroxy-group, in the transient cation radical, is coupled with intramolecular electron transfer furnishing the O-centered radical, which subsequently fragments. The quantum yields of fragmentation increase for higher alkyl substituted dithiane adducts.

1. Introduction

Heteroatom-centered cation radicals, C_β–C_α–$X^{\bullet+}$, which are readily generated by photoinduced electron transfer (ET), are subject to mesolytic fragmentation. It is well known that removal of one electron from the heteroatom's lone pair in the ground state significantly reduces the bond order of the geminal bonds, which either increases the acidity of the alpha-proton (H–C_α) or causes the C_α–C_β bond to cleave. In our previous work we utilized this increased acidity of the alpha-proton and developed an efficient electrochemical deprotection for carboxylates in general, and amino acids in particular, based on esters of hydroxymethyldithiane.[1] In this paper we will focus primarily on photoinduced C–C bond fragmentations in adducts of dithianes with ketones.

ET-induced fragmentations in vicinal amino alcohols and diols have been extensively studied.[2] The accepted mechanistic rationale includes photoinduced electron transfer to an ET-sensitizer, e.g., benzophenone, followed by a mesolytic cleavage of the generated cation radical, assisted by the benzophenone anion radical deprotonating the vicinal hydroxy group. It was noted that the C–C bond cleavage step is reminiscent of the Grob fragmentation in closed shell systems.[3]

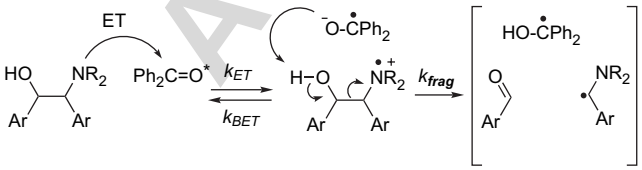

One of the early examples by Whitten and Ci involved thioindigo-sensitized fragmentation in the *threo*- and *erythro*-2-morpholino-1,2-diphenylethanol.[3a] Assuming that the only temperature-dependent process in the reaction of the geminate ion radical pair is k_{frag}, they determined the Arrhenius activation energy for the *threo*- and *erythro* diastereomers to be 4.9 and 2.8 kcal/mol, respectively. This demonstrates a strong conformational dependence of the cleavage and shows that the activation barrier is very low.

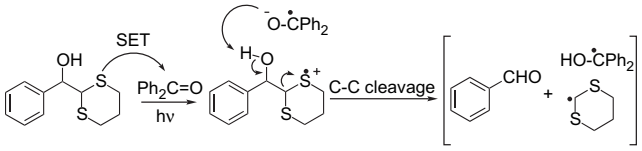

Similar reactions of sulfido-alcohols are also known. For example, Gravel et al. utilized the C–C cleavage in β-phenylthioalkanols as a synthetic method for indirect cleavage of olefins[4] and also in carbohydrate synthesis.[5] Some time ago we found that dithianes are particularly suitable for this chemistry: their adducts are readily synthesized and they cleave efficiently upon photoinduced fragmentation. The mechanism of cleavage in dithiane adducts was investigated by utilizing classical physical organic methods such as the Hammett substituent effect, the kinetic isotope effect,[6] and laser flash photolysis studies.[7] Our initial mechanistic findings were in keeping with the universally recognized 'Grob-like' mechanism, until we tested the photoinduced fragmentation in the *tert*-butyl derivative **A**, which in addition to the expected pivalaldehyde **B** ('normal' cleavage) produced dithiane-2-carboxaldehyde **C** as a major product in 1:6.2 ratio.[8] It became clear that the quasi-Grob electron

* Corresponding author. E-mail: akutatel@du.edu

0040–4020/$ - see front matter © 2006 Elsevier Ltd. All rights reserved.
doi:10.1016/j.tet.2006.03.065

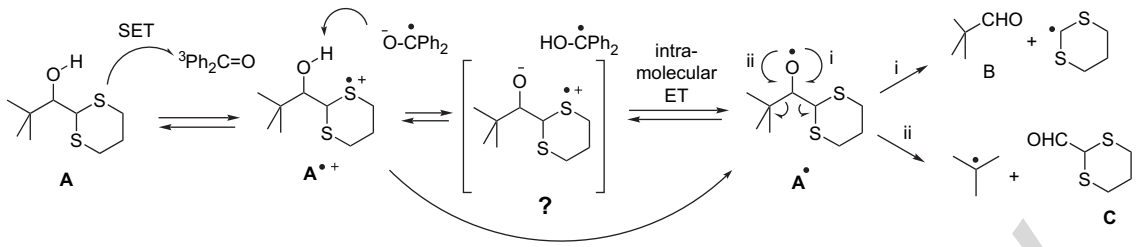

Scheme 1.

pushing rationale needed refinement because adduct **A** was primarily cleaving the wrong bond.

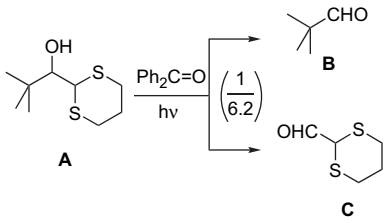

Further experimental and computational investigation suggested that deprotonation of the hydroxy group in the initially generated cation radical does not result in the formation of a charge separated 'Grob-like' precursor $^-$O–C–C–$S^{+\bullet}$–R, but rather produces a neutral oxygen-centered radical (or a species behaving as one) via intramolecular electron transfer. The O-centered radical undergoes subsequent fragmentation in either direction and the partitioning correlates with stability of the produced radicals, Scheme 1.[9] When methyldithiane derivative **D** was used in place of **A**, the ratio of **B**:**C**=1:6.2 was inverted to become **B**:**E**=1.8:1, all in keeping with relative stability of *tert*-butyl, dithian-2-yl, and 2-methyldithian-2-yl radicals. We also compared the

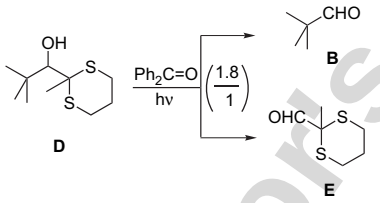

results of the fragmentation in methylene chloride and acetonitrile, which constitutes almost an order of magnitude difference in the dielectric constant, and did not see any difference in the partitioning within experimental error. All these results seem to indicate that the charge separated species does not exist, or at best it is in fast equilibrium with the alkoxy radical (Scheme 1).

The case of *tert*-butyl derivatives, such as **A** and **D**, is unique in a sense that it allowed us to discover this new channel in the mechanism of fragmentation simply by product analysis. For dithiane adducts of aromatic aldehydes and ketones the barrier for the aryl radical departure is prohibitively high, i.e., it is the dithiane radical, which is *always* departing. Therefore, it is much more difficult to ascertain whether or not the original Grob-like mechanism for cleavage competes with the anomalous O-centered radical mechanism (or either one of them is operating exclusively) in the case of aromatic adducts. Because of the presence of sulfur it is synthetically challenging, if not impossible, to generate the O-radical $\mathbf{A}^{\bullet}$ from an alternative precursor, for example, a peroxide, and study the effect of substituents on the rate of its degradation.

In this paper we report our experimental and computational study of the mechanism of photoinduced cleavage in adducts of 2-alkyl substituted dithianes with benzophenone, which is intended to further refine the mechanism of fragmentation. Benzophenone-sensitized mesolytic fragmentations, in adducts of the sensitizer itself, result in generation of more benzophenone and, as such, constitute its amplification. Hence, our particular interest in this system, which we plan to utilize in various photochemical applications.

2. Results and discussion

Benzophenone adducts **2a**–**e** of unsubstituted (**1a**), 2-methyl- (**1b**), 2-ethyl- (**1c**), 2-hexyl (**1d**), and 2-decyl (**1e**) dithiane were synthesized according to a modified Corey–Seebach procedure[10] (Scheme 2) and their photoinduced fragmentation was studied over a temperature range from −40 to +40 °C in acetonitrile upon benzophenone sensitization. The driving force for the oxidative electron transfer from the dithiane moiety to the triplet state of benzophenone in acetonitrile is rather large: the one electron reduction potential of triplet benzophenone is −1.68 V (vs SCE in acetonitrile),[11] whereas various 2-substituted dithianes oxidize in the range of +0.73 to +1.18 V in the same solvent.[12] During the course of a laser flash photolysis study[7] we found that the rate of initial electron transfer quenching of triplet benzophenone with dithiane–benzophenone adduct in dry acetonitrile was near the diffusion limit, $8.4\pm0.7\times10^8$ M^{-1} s^{-1}. In 10% aqueous acetonitrile the quenching rate was even higher, $1.31\pm0.06\times10^9$ M^{-1} s^{-1}. In the present study we have determined the dependence of the quantum efficiency of fragmentation on temperature and compared the experimental (apparent) activation enthalpy with the calculated activation barrier for the β-scission in the corresponding

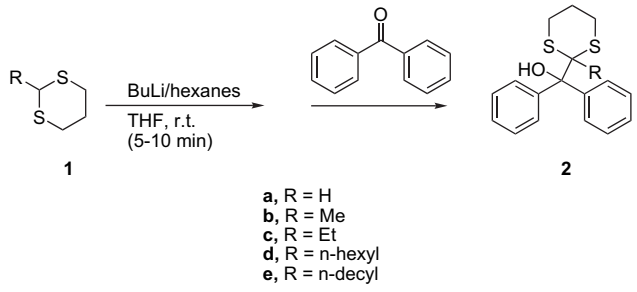

Scheme 2.

Table 1. Quantum efficiencies and dithiane recovery rates at +20 °C for adducts **2b–e**

Adduct	ϕ	Dithiane recovery (%)
Methyl- (**2b**)	0.20	32.8
Ethyl- (**2c**)	0.23	35.3
Hexyl- (**2d**)	0.25	41.0
Decyl- (**2e**)	0.27	47.8

O-centered radicals. The computations were run at the DFT, B3LYP/6-31G(d), level using Gaussian 03, revision C.02.[13]

Photolyses were carried out in a carousel Rayonet photoreactor with a Pyrex heat exchange jacket cooled by ethanol circulating through a FTS Systems Multi-Cool refrigeration unit. The quantum yield determinations were done using the classic benzophenone—benzhydrol actinometer system as a standard.[14] Having benzophenone as a common sensitizer, in both the photoinduced fragmentation under study and the actinometer system, significantly improves the accuracy of quantum yield determinations. In addition to the overall quantum yield of adduct disappearance another important parameter is the percent recovery of the corresponding dithiane. Both the Grob-like and the O-centered radical mechanisms have a dithian-2-yl radical as the immediate fragmentation product. Its fate depends on multiple factors, including the reactivity of such a radical towards oxygen, dimerization, disproportionation etc. The recovery of dithiane in turn depends on all of the above and also on the rate of its degradation as a result of secondary photooxidation by benzophenone. We found that more substituted dithianes showed better recovery, which is in agreement with the overall trends in reactivity of the dithian-2-yl radicals (i.e., unsubstituted dithianyl radicals react/degrade faster) and of the final products—dithianes (i.e., less substituted dithianes undergo benzophenone-sensitized oxidative photodegradation faster). The quantum efficiency of cleavage also steadily increases for adducts of dithianes substituted with longer alkyl chains (Table 1).

Table 2. Quantum yields of fragmentation and % dithiane recovery as a function of temperature

T (°C)	Ethyl adduct **2c**		Methyl adduct **2b**	
	ϕ	Dithiane recovery (%)	ϕ	Dithiane recovery (%)
−40	0.04	0.7	0.01	1.5
−20	0.13	6.2	0.05	4.3
0	0.18	17.8	0.10	6.2
20	0.21	14.8	0.15	8.7
40	0.32	37.6	0.25	12.5

The adduct of the parent compound, unsubstituted dithiane, showed poor efficiency of cleavage. This deficiency is not due to the impediment of the initial electron transfer: our previous LFP experiments show that the initial electron transfer quenching rate increases with the decreased substitution.[7] It is difficult to argue definitively about the partitioning of the initially formed dithiane cation radical—benzophenone anion radical pair (i.e., the partition between the back electron transfer and the productive deprotonation of the adduct by the anion radical leading to fragmentation). However, following Whitten's assumption[3a] that the only temperature-dependent process in a reaction of the geminate radical ion pair is fragmentation, we obtained the enthalpy of activation by plotting the data shown in Table 2 as $\log(\phi/T)$ versus $1/T$ for the reaction of **2b** and **2c** (Fig. 1).

The activation enthalpies, $\Delta H^{\neq}$, are obtained from the slopes: 4.7 kcal/mol for the methyl derivative **2b** and 1.5 kcal/mol for the ethyl derivative **2c** (Fig. 1a). These values are very similar to the activation energies obtained by Whitten for the thioindigo-sensitized fragmentation in vicinal amino alcohols.[3a]

We suggest that the effect of substitution at position 2 of dithiane reflects largely the acceleration of the fragmentation in the deprotonated species, the oxygen-centered radical. Walling and Padwa[15] studied the substitution effect in decomposition of hypochlorites of alkyldimethylcarbinols, R–C(Me)$_2$–O–Cl, by comparing the differences in activation energies for decomposition and hydrogen abstraction. They reported that while the difference was 10 kcal/mol for *tert*-butoxy radical (i.e., R=Me), it decreased to 1.7 for R=*i*-Pr, 0.7 for R=benzyl, and was negligibly small for R=*t*-Bu. The absolute value for the activation energy of fragmentation in *tert*-butoxy radical is 11–13 kcal/mol.[16] Assuming that the rate of hydrogen abstraction does not change much, introduction of the *tert*-butyl group in place of methyl should lower the activation energy of fragmentation in these alkoxy radicals by about 10 kcal/mol, to approx. 1–3 kcal/mol. 2-Methyl-1,3-dithian-2-yl and 2-ethyl-1,3-dithian-2-yl are very stable (and bulky) radicals. Judging by our previous observations of the competitive cleavage, the 2-methyldithianyl radical is more stable than *tert*-butyl, which in turn is more stable than the unsubstituted dithiane-2-yl radical.[8] Summarizing these arguments, it is

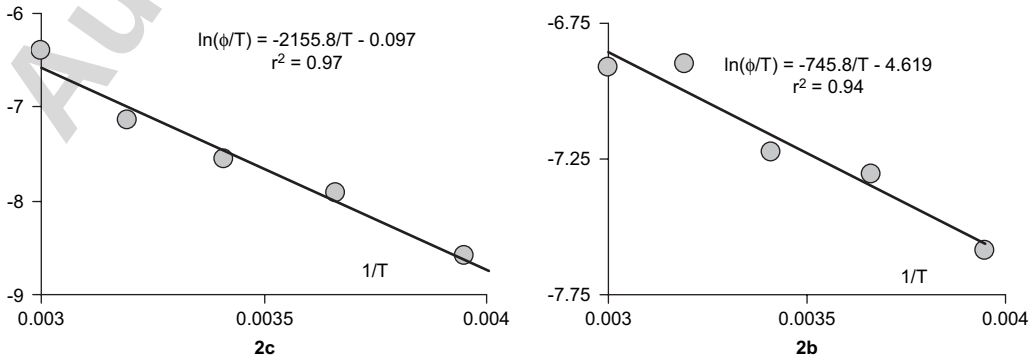

Figure 1. $1/T$ dependence of fragmentation quantum yields for ethyl (**2c**) and methyl (**2b**) adducts.

Table 3

	SS (kcal/mol)	TS (kcal/mol)	$\Delta H^{\neq}$ (kcal/mol)
Ethyl-derivative ***2c•*** *(O-radical)*			
aEaO-**2c•**	5.4	10.2	4.77
aEgO-**2c•**	4.5	22.6	18.15
eEaO-**2c•**	1.1	[a]	—
eEgO-**2c•**	0.0	1.7	1.70
Methyl derivative ***2b•*** *(O-radical)*			
aMaO-**2b•**	3.4	8.5	5.05
aMgO-**2b•**	2.8	5.1	2.24
eMaO-**2b•**	0.9	[a]	—
eMgO-**2b•**	0.0	1.7	1.72

[a] Computations did not converge.

not unreasonable to assume that the apparent $\Delta H^{\neq}$ of 4.7 and 1.5 kcal/mol, obtained in this study, correspond to fragmentation in the oxygen-centered radicals, expelling methyldithianyl and ethyldithianyl radicals, respectively.

To support this hypothesis we carried out DFT computations at a B3LYP/6-31G(d) level, using the whole untruncated structures of the methyl- and ethyldithiane adducts of benzophenone (**2b** and **2c**). The initial geometries of the respective oxygen-centered radicals (**2b•** and **2c•**) were generated with Chem3D and pre-optimized at the AM1 level. Vibrational analysis of the DFT optimized geometries show no imaginary frequencies for the computed minima (ground states) and only one imaginary frequency for the transition states corresponding to the reaction coordinate (i.e., C–C stretch). Given the importance of conformational considerations, we scanned the conformational space and analyzed the relative energies of the starting alkoxy radicals and their respective fragmentation transition states for the four major conformers: (i) equatorial 2-alkyl with the CO bond in *anti* conformation to this alkyl, denoted eMaO, i.e., *e*quatorial *M*ethyl *a*nti *O*xygen (the oxygen is *anti* to the methyl group), and eEaO for *E*thyl; (ii) equatorial 2-alkyl—*gauche* CO bond, eMgO/eEgO; (iii) axial 2-alkyl—*anti* CO bond; aMaO/aEaO; (iv) axial 2-alkyl—*gauche* CO bond, aMgO/aEgO. The other two sets of the *gauche* conformers are enantiomers of eMgO/eEgO and aMgO/aEgO. The relative energies of the starting oxy-radicals and their respective transition states are listed in Table 3 with the calculated $\Delta H^{\neq}$ summarized in the third column.

Strikingly, the lowest energy conformations for both methyl and ethyl derivatives had the smaller alkyl substituent in the equatorial position, whereas the bulky benzhydryl group was axial, with oxy-radical being *gauche* to methyl/ethyl (i.e., *anti* to one of sulfur atoms). The transition state geometries were obtained at the same B3LYP/6-31G(d) level of theory. The electronic energies for all the species in Table 3 are zpe-corrected. As follows from the table, the eMgO/eEgO conformers have the lowest energies both at the minima and the transition states (see also Fig. 2). This is also in keeping with the computed conformational energies of the parent alcohols that showed at least a 2 kcal/mol preference for the eRgO conformers (Table 4).

Table 4. DFT relative energies for the conformers of alcohols **2a–c**

Conformers	Rel energy (kcal/mol)
aMaO-**2b**	3.15
aMgO-**2b**	3.45
eMaO-**2b**	2.90
eMgO-**2b**	0.00
aEaO-**2c**	5.52
aEgO-**2c**	1.91
eEaO-**2c**	3.18
eEgO-**2c**	0.00
aHaO-**2a**	0.01
aHgO-**2a**	0.00
eHaO-**2a**	3.31
eHgO-**2a**	2.80

On the contrary, for the C-2 unsubstituted dithiane adduct it was the axial-H (i.e., the equatorial benzhydrol) conformers aHaO and aHgO that were expectedly more stable by approx. 3 kcal/mol.

NMR spectroscopic study of the parent alcohols supported the DFT findings. The initial analysis of the 1D proton NMR spectra of the three adducts shows systematic upfield shift of the dithiane's $H_2C^{(3)}$ and $H_2C^{(5)}$ protons upon introduction of the methyl and then ethyl group. The downfield multiplet corresponds to two axial $H_2C^{(3)}$ and $H_2C^{(5)}$ protons and the upfield—equatorials (Fig. 3).

Low temperature NMR data show dramatic differences in conformational behavior of the substituted (**2b** and **2c**) versus unsubstituted (**2a**) derivatives. The temperature-dependent changes in one-dimensional ^1H NMR spectra are shown in Figure 4. Below −40 °C the multiplets for both axial and equatorial protons $H_2C^{(3)}$ and $H_2C^{(5)}$ in the Me- and Et-derivatives split into two sets. It appears that the

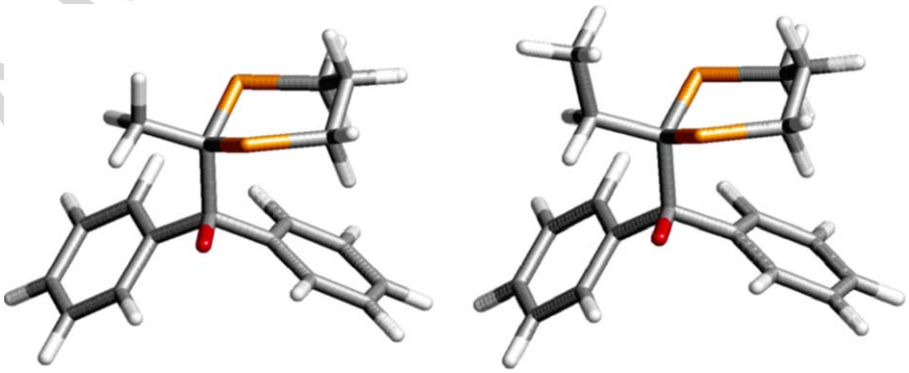

Figure 2. The lowest energy conformers of the respective O-centered radicals: eMgO-**2b•** (left) and eEgO-**2c•** (right).

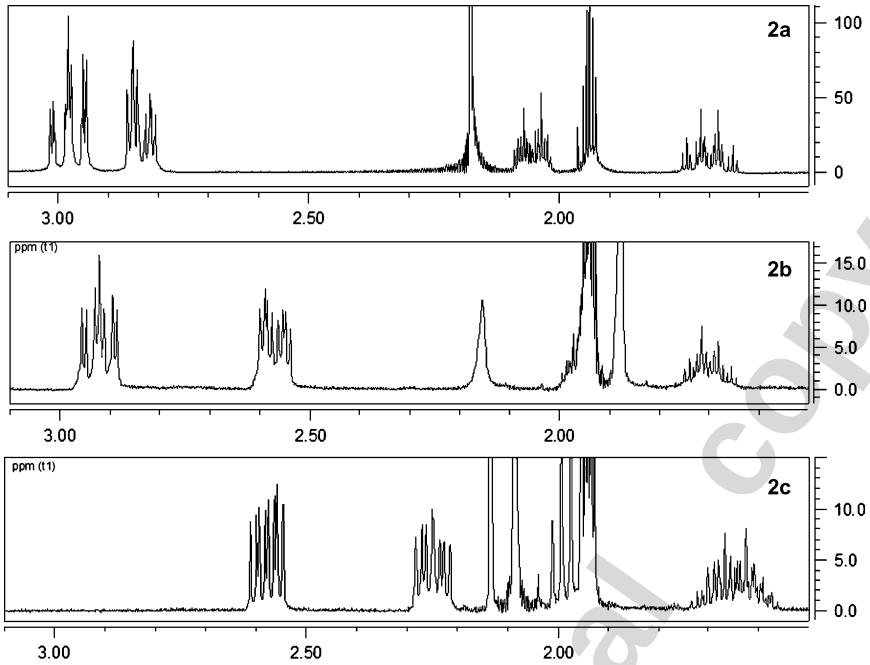

Figure 3. 1D proton NMR spectra of **2a–c**.

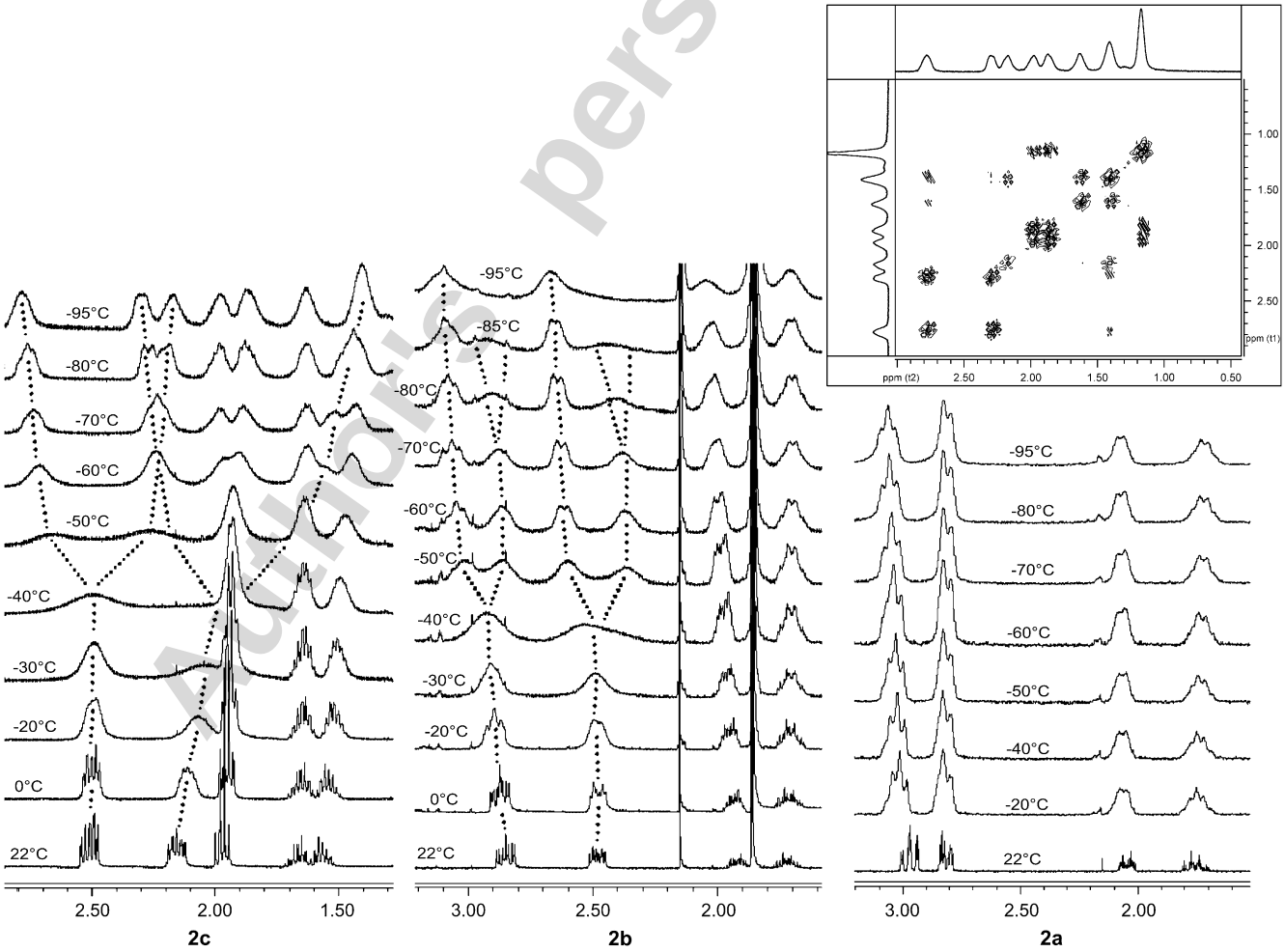

Figure 4. VT NMR data for **2a–c**. The inset shows low temperature COSY spectrum for **2c** at −95 °C.

rotation of the benzhydryl group is stopped at this temperature and that the most stable isomer is unsymmetrical.

On the contrary, NMR spectrum of unsubstituted **2a** shows negligible temperature-dependent changes, which could indicate that the most stable conformer is symmetric (i.e., *anti*). An alternative interpretation is that the rotation of the benzhydrol group is not stopped even at −95 °C in unsubstituted **2a**.

Equal integrated intensities of the split signals of the equatorial and axial protons indirectly confirm that they belong to the same conformer, not to two frozen populations of conformers, e.g., chair-to-chair, or chair–twist conformers of dithiane, in which case they would be expected to have different integrated values. For more definitive assignment, we ran a COSY experiment of **2c** at −95 °C, which unambiguously showed strong cross-peaks for the respective split pairs of signals. We therefore conclude, that below −40 °C both equatorial protons H_{eq}–$C^{(3)}$ and H_{eq}–$C^{(5)}$ of the dithiane ring are not equivalent and separate into two signals. The same is true for the pair of axial protons H_{ax}–$C^{(3)}$ and H_{ax}–$C^{(5)}$. These data can only be explained in terms of asymmetric conformation of the frozen benzhydrol group, which is in keeping with our computational finding that the asymmetric eRgO conformers are the most stable. The low temperature data for the Me derivative **2b** in Figure 4 show some additional line broadening for each of the upfield (right) signals of the split peaks, indicating that another degree of freedom is being frozen at −60 °C and below. We do not have an immediate explanation for this behavior—there can be a number of conformational processes that can cause the observed coalescence of signals at this temperature.

In conclusion, the measured apparent enthalpies of activation for photoinduced fragmentation in the alkyl dithiane–benzophenone adducts are in keeping with the kinetic barriers computed at the B3LYP/6-31G(d) level of theory for the mechanism involving formation of an alkoxy radical and its subsequent fragmentation. The findings do not rule out the charge separated Grob-like mechanism, but rather provide new evidence to support an alternative nonpolar mechanism. As to the design and development of the dithiane-based photolabile latches: utilization of higher alkyls at position 2 of dithiane increases both the quantum yield of fragmentation and recovery of dithiane, attesting to the potential of longer alkyl chains as a promising alternative for the molecular design of efficient photolabile tethers.

3. Experimental

3.1. General

Common solvents were purchased from Pharmco and used as is, except for THF, which was refluxed over and distilled from potassium benzophenone ketyl prior to use. *n*-BuLi (as a 1.6 M solution in hexane), 1,3-dithiane, 2-methyl-1,3-dithiane, benzophenone, and benzhydrol were purchased from Aldrich. 1,3-Dithiol was purchased from Acros. Propanal, decanal, and heptanal were purchased from Alfa Aesar. All reagents were used without purification. ^{1}H NMR spectra were recorded at 25 °C on a Varian Mercury 400 MHz instrument in $CDCl_3$ with TMS as an internal standard (unless noted otherwise). Low temperature NMR was carried out in CD_3OD using a Varian Mercury VT system. Temperature was controlled using dry nitrogen flow through a liquid nitrogen Dewar. Column chromatography was performed on silica gel, 70–230 mesh ASTM, using ethyl acetate–hexane mixtures as eluent. Photoreactions were carried out in the carousel Rayonet photoreactor outfitted with a jacketed Pyrex reaction vessel connected to a FTS Systems Multi-Cool refrigeration unit with a peristaltic pump, using ethanol as a coolant.

Ab initio computations were performed on a Linux workstation using Gaussian 03, Revision C.02.[13] Input geometries were created and pre-optimized using a force field geometry optimization as implemented in Chem3D (Cambridgesoft). The geometries were further pre-optimized at the AM1 level. Full geometry optimizations were performed using density functional theory (DFT) at the B3LYP/6-31G(d) level of theory (the Becke three-parameter hybrid functional combined with Lee, Yang, and Parr correlation functional[17]).

3.2. General method for dithiane preparation

1,3-Propanedithiol (0.07 mol) and the appropriate aldehyde (0.06 mol) were dissolved in 250 mL CH_2Cl_2. $BF_3 \cdot Et_2O$ (0.26 mol) was added to the solution. The reaction mixture was then stirred overnight at room temperature. The mixture was washed with NaOH (5% aq soln) and water. The organic layer was dried over anhydrous $NaSO_4$ and the solvent was removed by rotary evaporator and the resulting product was distilled under vacuum.

3.2.1. 2-Ethyl-1,3-dithiane (1c). Yield 8.7 g, 59 mmol, 86%; bp 38 °C/63 mTorr; ^{1}H NMR (CDCl3, 400 MHz): δ 4.0 (t, 1H, J=6.8 Hz), 2.80–2.92 (m, 4H), 2.09–2.16 (m, 1H), 1.84–1.92 (m, 1H), 1.77–1.92 (m, 2H), 1.09 (t, 3H).

3.2.2. 2-Hexyl-1,3-dithiane (1d). Yield 5.4 g, 26 mmol, 54%; bp 125 °C/72 mTorr; ^{1}H NMR ($CDCl_3$, 400 MHz): δ 4.03 (t, 1H, J=6.9 Hz), 2.76–2.90 (m, 4H), 2.06–2.13 (m, 1H), 1.83–1.92 (m, 1H), 1.68–1.74 (m, 2H), 1.44–1.52 (m, 2H), 1.22–1.35 (m, 6H), 0.87 (t, 3H).

3.2.3. 2-Decyl-1,3-dithiane (1e). Yield 12.56 g, 48 mmol, 63%; bp 142 °C/69 mTorr; ^{1}H NMR ($CDCl_3$, 400 MHz): δ 4.07 (t, 1H, J=6.9 Hz), 2.81–2.94 (m, 4H), 2.10–2.17 (m, 1H), 1.85–1.94 (m, 1H), 1.73–1.79 (m, 2H), 1.48–1.55 (m, 2H), 1.25–1.33 (m, 14H), 0.90 (t, 3H).

3.3. General method for adduct preparation

A generic method by Corey and Seebach was modified and used to prepare the desired dithiane–benzophenone adducts.[10] Dithiane (5.1 mmol) was dissolved in freshly distilled THF (30 mL) and placed under nitrogen. *n*-Butyllithium (4.3 mL, 6.8 mmol) was added at room temperature upon stirring and the resulting mixture was stirred for 10 more minutes. Benzophenone (3.4 mmol) was dissolved in freshly distilled THF (10 mL) and added to the anion mixture with stirring. The reaction was left overnight. The reaction mixture was quenched with a saturated solution of ammonium chloride and the aqueous layer was extracted

twice with ethyl acetate. The combined organic layer was dried over anhydrous sodium sulfate. The solvent was removed with a rotary evaporator, and the residue was purified by column chromatography (silica gel, ethyl acetate–hexane) or recrystallization (methanol).

3.3.1. (2-Methyl-[1,3]-dithian-2-yl)-diphenyl-methanol (2b). Yield 0.80 g, 2.7 mmol, 80%; ^{1}H NMR ($CDCl_3$, 400 MHz): δ 7.85–7.87 (m, 4H), 7.21–7.30 (m, 6H), 2.82 (ddd, 2H, J=3.5, 10.5, 14.6 Hz), 2.53 (ddd, 2H, J=3.9, 5.7, 14.7 Hz), 1.80–1.97 (m, 2H), 1.894 (s, 3H).

3.3.2. (2-Ethyl-[1,3]-dithian-2-yl)-diphenyl-methanol (2c). Yield 0.94 g, 2.8 mmol, 93%; ^{1}H NMR ($CDCl_3$, 400 MHz): δ 7.93–7.96 (m, 4H), 7.28–7.33 (m, 4H), 7.22–7.26 (m, 2H), 2.52 (ddd, 2H, J=4.8, 7.0, 14.2 Hz), 2.25 (ddd, 2H, J=4.8, 8.1, 13.0 Hz), 1.97–2.04 (m, 2H), 1.67–1.73 (m, 2H), 1.12–1.16 (m, 3H).

3.3.3. (2-Hexyl-[1,3]-dithian-2-yl)-diphenyl-methanol (2d). Yield 0.61 g, 1.6 mmol, 49%; ^{1}H NMR ($CDCl_3$, 400 MHz): δ 7.91–7.94 (d, 4H), 7.20–7.31 (m, 6H), 2.49 (td, 1H, J=4.8, 10.3 Hz), 2.22 (ddd, 1H, J=5.9, 8.0, 14.1 Hz), 1.91–1.96 (m, 2H), 1.60–1.73 (m, 4H), 1.10–1.31 (m, 6H), 0.81–0.85 (t, 3H).

3.3.4. (2-Decyl-[1,3]-dithian-2-yl)-diphenyl-methanol (2e). Yield 0.62 g, 1.4 mmol, 52%; ^{1}H NMR ($CDCl_3$, 400 MHz): δ 7.92–7.94 (dd, 4H), 7.20–7.33 (m, 6H), 2.49 (td, 2H, J=5.4, 14.1 Hz), 2.23 (ddd, 1H, J=5.7, 8.2, 13.9 Hz), 1.91–1.96 (m, 2H), 1.60–1.77 (m, 6H), 1.10–1.34 (m, 12H), 0.81–0.85 (t, 3H).

Acknowledgements

Support for this research by the National Science Foundation (CHE-314344) is gratefully acknowledged.

References and notes

1. Barnhurst, L. A.; Wan, Y.; Kutateladze, A. G. *Org. Lett.* **2000**, *2*, 799.
2. For review see: Gaillard, E. R.; Whitten, D. G. *Acc. Chem. Res.* **1996**, *29*, 292.
3. (a) Ci, X.; Whitten, D. G. *J. Am. Chem. Soc.* **1987**, *109*, 7215; (b) Ci, X.; Whitten, D. G. *J. Am. Chem. Soc.* **1989**, *111*, 3459.
4. Gravel, D.; Farmer, L.; Ayotte, C. *Tetrahedron Lett.* **1990**, *31*, 63.
5. Gravel, D.; Farmer, L.; Denis, R. C.; Schultz, E. *Tetrahedron Lett.* **1994**, *35*, 8981.
6. McHale, W. A.; Kutateladze, A. G. *J. Org. Chem.* **1998**, *63*, 9924.
7. Vath, P.; Falvey, D. E.; Barnhurst, L. A.; Kutateladze, A. G. *J. Org. Chem.* **2001**, *66*, 2886.
8. Li, Z.; Kutateladze, A. G. *J. Org. Chem.* **2003**, *68*, 8236.
9. β-Alkylthio-ethoxy radicals were implicated in the dissociation of hydroxyl radical adducts of (alkylthio)ethanol derivatives: Schöneich, C.; Bobrowski, K. *J. Am. Chem. Soc.* **1993**, *115*, 6538.
10. Seebach, D.; Corey, E. J. *J. Org. Chem.* **1975**, *30*, 231.
11. Roth, H. D.; Lamola, A. A. *J. Am. Chem. Soc.* **1974**, *96*, 6270.
12. Glass, R. S.; Petsom, A.; Wilson, G. S. *J. Org. Chem.* **1986**, *51*, 4337.
13. Frisch, M. J.; Trucks, G. W.; Schlegel, H. B.; Scuseria, G. E.; Robb, M. A.; Cheeseman, J. R.; Montgomery, J. A., Jr.; Vreven, T.; Kudin, K. N.; Burant, J. C.; Millam, J. M.; Iyengar, S. S.; Tomasi, J.; Barone, V.; Mennucci, B.; Cossi, M.; Scalmani, G.; Rega, N.; Petersson, G. A.; Nakatsuji, H.; Hada, M.; Ehara, M.; Toyota, K.; Fukuda, R.; Hasegawa, J.; Ishida, M.; Nakajima, T.; Honda, Y.; Kitao, O.; Nakai, H.; Klene, M.; Li, X.; Knox, J. E.; Hratchian, H. P.; Cross, J. B.; Adamo, C.; Jaramillo, J.; Gomperts, R.; Stratmann, R. E.; Yazyev, O.; Austin, A. J.; Cammi, R.; Pomelli, C.; Ochterski, J. W.; Ayala, P. Y.; Morokuma, K.; Voth, G. A.; Salvador, P.; Dannenberg, J. J.; Zakrzewski, V. G.; Dapprich, S.; Daniels, A. D.; Strain, M. C.; Farkas, O.; Malick, D. K.; Rabuck, A. D.; Raghavachari, K.; Foresman, J. B.; Ortiz, J. V.; Cui, Q.; Baboul, A. G.; Clifford, S.; Cioslowski, J.; Stefanov, B. B.; Liu, G.; Liashenko, A.; Piskorz, P.; Komaromi, I.; Martin, R. L.; Fox, D. J.; Keith, T.; Al-Laham, M. A.; Peng, C. Y.; Nanayakkara, A.; Challacombe, M.; Gill, P. M. W.; Johnson, B.; Chen, W.; Wong, M. W.; Gonzalez, C.; Pople, J. A. *Gaussian 03, Revision C.02*; Gaussian: Wallingford, CT, 2004.
14. Moore, W. M.; Hammond, G. S.; Foss, R. P. *J. Am. Chem. Soc.* **1961**, *83*, 2789.
15. Walling, C.; Padwa, A. *J. Am. Chem. Soc.* **1963**, *85*, 1593.
16. Gray, P.; Williams, A. *Chem. Rev.* **1959**, *59*, 239.
17. (a) Becke, A. D. *Phys. Rev. A* **1988**, *38*, 3098; (b) Lee, C.; Yang, W.; Parr, R. G. *Phys. Rev. B* **1988**, *37*, 785.